Engineering Geology 155 (2013) 31–44

Contents lists available at SciVerse ScienceDirect

Engineering Geology

journal homepage: www.elsevier.com/locate/enggeo

Mountain torrents: Quantifying vulnerability and assessing uncertainties

Reinhold Totschnig [a,b,*], Sven Fuchs [a,c]

[a] Institute of Mountain Risk Engineering, University of Natural Resources and Life Sciences, Peter-Jordan-Straße 82, 1190 Vienna, Austria
[b] eb&p Umweltbüro GmbH, Bahnhofstraße 39/2, 9020 Klagenfurt, Austria
[c] Faculty of Geography, Lomonosov Moscow State University, Leninskie gory 1, 119991 Moscow, Russian Federation

ARTICLE INFO

Article history:
Received 26 June 2012
Received in revised form 21 December 2012
Accepted 29 December 2012
Available online 17 January 2013

Keywords:
Quantitative risk assessment
Vulnerability
Mountain hazards
Uncertainties
Validation
European Alps

ABSTRACT

Vulnerability assessment for elements at risk is an important component in the framework of risk assessment. The vulnerability of buildings affected by torrent processes can be quantified by vulnerability functions that express a mathematical relationship between the degree of loss of individual elements at risk and the intensity of the impacting process. Based on data from the Austrian Alps, we extended a vulnerability curve for residential buildings affected by fluvial sediment transport processes to other torrent processes and other building types. With respect to this goal to merge different data based on different processes and building types, several statistical tests were conducted. The calculation of vulnerability functions was based on a nonlinear regression approach applying cumulative distribution functions. The results suggest that there is no need to distinguish between different sediment-laden torrent processes when assessing vulnerability of residential buildings towards torrent processes. The final vulnerability functions were further validated with data from the Italian Alps and different vulnerability functions presented in the literature. This comparison showed the wider applicability of the derived vulnerability functions. The uncertainty inherent to regression functions was quantified by the calculation of confidence bands. The derived vulnerability functions may be applied within the framework of risk management for mountain hazards within the European Alps. The method is transferable to other mountain regions if the input data needed are available.

1. Introduction

Natural hazards, such as snow avalanches, landslides and torrent processes, pose a threat to the urban development and infrastructure in mountain areas. The adverse effects associated with these hazards may increase due to the continued socio-economic development in some mountain regions and the possible influence of climate change on the frequency and magnitude of the hydro-geomorphic processes (Cendrero et al., 2006; Jakob and Lambert, 2009; Keiler et al., 2010). For decades, geohazard assessments focused on the hazard potential of mass movements and corresponding mitigation strategies (Merz, 2006; Holub and Fuchs, 2009). This evolved into a risk-based approach (e.g., Kienholz et al., 2004). The concept of risk represents a possibility to address mountain hazards and their potential consequences based on a common framework, normally referred to as risk or disaster management (Carter, 1992; Alexander, 2000; Kienholz et al., 2004). Vulnerability assessment for elements at risk (e.g., buildings located on torrent fans) is an important component in this risk-based approach (Uzielli et al., 2008; Fuchs, 2009; Fuchs et al., 2012). Vulnerability is thereby defined as the degree of loss of a given element at risk as a result from the occurrence of a natural phenomenon of a given intensity, ranging between 0 (no damage) and 1 (total loss) (UNDRO, 1979; Fell et al., 2008). Several methods to assess vulnerability have been proposed, and these assessment methods can be qualitative, semi-quantitative, or quantitative (Fuchs et al., 2011). With respect to mountain hazards, the quantification of vulnerability through the development and application of respective functional relationships has emerged within the previous two decades. These functions express a mathematical relationship between the intensity of the process and the degree of loss of the elements at risk. They are referred to either as vulnerability function (e.g., Fuchs et al., 2007a), vulnerability curve (e.g., Barbolini et al., 2004), damage function (e.g., FEMA, 2007) or fragility curve (e.g., Tsao et al., 2010). Fragility curves, however, generally relate the intensity of the process to the probability of exceeding certain damage states or, in the case of protection measures, states of failure (Merz, 2006; Schultz et al., 2010).

In this section, we summarise the different approaches dealing with vulnerability functions for torrent processes in chronological order.

Borter (1999a) reported a comprehensive approach for risk analyses focussing mainly on gravitational mass movements in the European Alps. Vulnerability functions were presented in this study for snow avalanches and rock fall processes (Borter, 1999b). With respect to floods and debris flows, however, vulnerability values were only given in tabular form for three classes (low, medium, high process intensity).

* Corresponding author at: eb&p Umweltbüro GmbH, Bahnhofstraße 39/2, 9020 Klagenfurt, Austria. Tel.: +43 463516614 46.
E-mail address: reinhold.totschnig@umweltbuero.at (R. Totschnig).

0013-7952/$ – see front matter
http://dx.doi.org/10.1016/j.enggeo.2012.12.019

The intensity parameters were quantified according to BWW (1997): the flood intensity was given as a combination between flow depth and flow velocity times flow depth and the debris flow intensity was given as a combination between deposition depth and flow velocity (Table 1).

Romang (2004) compiled a study on the effectiveness and costs of torrent mitigation measures in Switzerland. Flooding with an undefined amount of transported sediment was the considered process. Vulnerability data were based on the ratio between losses incurred and the reinstatement values of buildings at risk in order to calculate the degree of loss of buildings exposed to torrent processes. The respective data were provided by the building insurer.[1] Due to the considerable range in the vulnerability data, Romang (2004) concluded that a vulnerability function was not deducible and therefore, only mean vulnerability values for certain process intensity classes were presented. These intensity classes were defined according to the Swiss guidelines (Table 1).

Fuchs et al. (2007a) presented a vulnerability function for debris flows based on the analyses of an event in the Austrian Alps. Due to missing information on flow velocities, the deposition depth was taken as a proxy for the process intensity. Deposition depth directly adjacent to the damaged buildings was assessed during a field campaign following the incident and classified in steps of 0.5 m. The degree of loss was calculated as the ratio between monetary damage and reconstruction value for each building which included brick masonry and concrete residential buildings. The losses were collected using information from the federal authorities. Since in Austria an obligatory building insurance against losses from natural hazards is not available so far, property losses are partly covered by a governmental fund.[2] Consequently, these losses were collected on an object level immediately after an event by professional judges. The reconstruction values were calculated using the volume of the buildings and averaged prices (€/m^3) according to the type of building. The resulting vulnerability curve was expressed by a second order polynomial function. Although based on a limited number of data points, Fuchs et al. (2007a) demonstrated the general applicability of such an approach to torrent processes.

Akbas et al. (2009) applied the approach outlined by Fuchs et al. (2007a) to a debris flow event in the Italian Alps. Deposition depth as the intensity parameter and the degree of loss were derived similarly, and information regarding eleven damaged and two destroyed buildings was used to develop a vulnerability function as a second order polynomial function. Compared to the vulnerability function of Fuchs et al. (2007a), the vulnerability function obtained in Akbas et al. (2009) showed a similar shape but a higher degree of loss. Overall, the vulnerability values derived by Fuchs et al. (2007a) were approximately 35% smaller than the ones derived by Akbas et al. (2009). The limited number of data points, however, precludes a robust statement regarding the uncertainties. Possible explanations could be differences in process characteristics and construction techniques or the inherent range of the applied method (Akbas et al., 2009).

Table 1
Classification of intensity parameters according to BWW (1997) based on flow depth d_f (m), deposition depth d_d (m) and flow velocity v_f (m/s).

Intensity class	Flood	Debris flow
low	$d_f < 0.5$ or $v_f \cdot d_f < 0.5$	Not assessed
medium	$2 > d_f > 0.5$ or $2 > v_f \cdot d_f > 0.5$	$d_d < 1$ or $v_f < 1$
high	$d_f > 2$ or $v_f \cdot d_f > 2$	$d_d > 1$ and $v_f > 1$

Calvo and Savi (2009) applied vulnerability functions within a debris flow risk assessment. Three different vulnerability functions were tested in this study: a) a vulnerability function for flood waves using flow depth as intensity parameter, b) a vulnerability function for avalanches based on impact pressure, and c) a vulnerability relationship developed by Faella and Nigro (2001a,b) for debris flows, taking into account both hydrostatic and hydrodynamic forces. The latter is based on a combination of flow depth and flow velocity as intensity parameter. The debris flow hazard was computed using a Monte Carlo procedure. Calvo and Savi (2009) concluded that the vulnerability function developed for debris flows yielded the most reliable results. However, the main source of uncertainty in their debris flow risk assessment approach was the vulnerability assessment (Calvo and Savi, 2009).

Tsao et al. (2010) presented a debris flow risk estimation approach for Taiwan (Republic of China). For brick masonry and concrete buildings they used the vulnerability function presented in Fuchs et al. (2007a). A second vulnerability function was derived for wooden and sheet-metal buildings which represent a common construction type in Taiwan. As debris flows may damage the interior of a building, Tsao et al. (2010) recommended the use of an individual vulnerability curve for home interiors.

As outlined by Fuchs et al. (2007a), the second order polynomial functions used in these approaches have to be limited to an upper and lower threshold as they yield economic gains for very small process intensities and a degree of loss > 1 for high process intensities. To overcome these shortcomings, Totschnig et al. (2011) modified the approach by taking three torrent events characterised by fluvial sediment transport processes as an example. Instead of a second order polynomial function, cumulative distribution functions were used which define the degree of loss as a dependent variable in a confined interval between 0 and 1. In a first step, deposition depth was used as the intensity parameter to characterise the hazard process. A so-called relative intensity was further introduced to consider the influence of different building heights (different number of storeys) on the degree of loss. This relative intensity was defined as a normalised parameter composed from a ratio between the deposition depth and the height of the affected building. The individual analysis of both intensity parameters had shown that the application of a relative intensity parameter improves the calculation.

Quan Luna et al. (2011) applied a numerical debris flow model to derive vulnerability functions. The vulnerability values derived by Akbas et al. (2009) were related to different intensity parameters using the software FLO-2D. Accumulation height, impact pressure, and kinematic viscosity were back-calculated as intensity parameters for each individual building on the torrent fan. The proposed vulnerability

[1] In Switzerland, 19 of 26 cantons conduct a mandatory insurance system for buildings, underwriting natural hazards damage unlimited until the legally certified reinstatement values of the buildings (Fuchs et al., 2007b). Those insurers are organised as independent public corporations based on cantonal law, and cover approximately 80% of all Swiss buildings with an insured value of around € 1.2 billion. Within the individual canton, each insurer operates as a monopolist regulated by public law. Apart from the insurance policies, the business segments include loss prevention and risk management. In this context, cantonal insurers perform a sovereign function, consulting municipalities in all concerns on building permits and spatial planning activities.

[2] In Austria, natural hazards are not subject to compulsory insurance. Apart from the inclusion of losses resulting from hail, pressure due to snow load, rock fall and sliding processes in an optional storm damage insurance, no standardised product is currently available on the national insurance market. Moreover, the terms of business of this storm damage insurance explicitly exclude coverage of damage due to avalanches, floods and inundation, debris flows, earthquakes and similar extraordinary natural events (Holub et al., 2011). Furthermore, according to the constitution of the Republic of Austria, catastrophes resulting from natural hazards do not fall under the national jurisdiction. Thus, the responsibility for an aid to repair damage resulting from natural hazards generally rests with the Federal States. However, the Austrian government enacted a law for financial support of the Federal States in case of extraordinary losses due to natural hazards in the aftermath of the avalanche winter in 1951. The so-called 'law related to the catastrophe fund' (Katastrophenfondsgesetz) is the legal basis for the provision of national resources for (a) preventive actions to construct and maintain torrent and avalanche control measures, and (b) financial aids for the Federal States to enable them to compensate individuals and private enterprises for losses due to natural hazards in Austria. The budget of the catastrophe fund originates from a defined percentage (since 1996: 1.1%) of the federal share on the income taxes, capital gains taxes, and corporation taxes. The annually prescribed maximum reserves amount to € 29 million (Republik Österreich, 1996).

curves were expressed by logistic functions, and had to be limited to an upper threshold due to the fact that they yielded a degree of loss > 1 for high process intensities. Within their extent of validity they obtained high coefficients of determination.

Lo et al. (2012) reported vulnerability functions for residential buildings affected by debris flows in Taiwan (Republic of China). Loss functions for the content and the structure of the building were separately calculated and subsequently merged to a general vulnerability function. Two types of buildings were distinguished based on the construction material used (brick and reinforced brick), considering the different resistance against debris flow impacts. The content loss function was based on a synthetic approach taking the total values of fixtures and fittings as loss proxy when the process intensity (expressed as deposition depth) inside the building affects the corresponding element. The structure loss was quantified using the deposition depth as intensity parameter. Loss values were estimated by using reconstruction expenses for the incurred damage, as no insurance data were available in Taiwan.

Papathoma-Köhle et al. (2012) highlighted the challenge of missing data for the deduction of vulnerability curves. To overcome this gap, a methodology was presented to calculate the total loss of a building by summing up expenses for the fixing costs (repair works) of different damage patterns. For example, the damage pattern "flooding of the basement" necessitates the following works: removal of furniture and equipment, drying, cleaning, re-plastering and painting of the inner walls, and potentially the installation of new doors and floors. The damage patterns were identified from previous events in corresponding photo documentations. The reconstruction value, necessary for the calculation of the degree of loss, was estimated by using the footprint of the building and regional standard prices (€/m^2) for different building sections such as living area, attic and basement. The methodology was tested for a debris flow event in the Italian Alps. Deposition depth was applied as the intensity parameter, and since information regarding the monetary compensation of the losses was available for this event a visual validation of the deduced vulnerability curve showed a satisfying consistency.

Totschnig and Fuchs (2012) compared vulnerability functions for fluvial sediment transport with vulnerability functions deduced for debris flows. To compare different vulnerability curves, the approach outlined in Totschnig et al. (2011) was applied during the set of calculations. The resulting vulnerability curves for fluvial sediment transport processes and debris flows exhibited a mismatch due to a data gap related to high loss values in case of debris flows. However, after complementing the debris flow data set with vulnerability values given in Akbas et al. (2009), the vulnerability curves for debris flow and fluvial sediment transport showed nearly the same shape. Hence, the authors concluded that there is no need to distinguish between different sediment-laden torrent processes when assessing the physical vulnerability of residential buildings.

Vulnerability functions are only one way to assess the vulnerability of buildings. Using semi-quantitative approaches, threshold values of impact pressure for different damage classes (Zanchetta et al., 2004; Hu et al., 2012) as well as qualitative intensity parameters for quantitative vulnerability values (Fell and Hartford, 1997; Bell and Glade, 2004) are suggested. Haugen and Kaynia (2008) adopted fragility curves developed for earthquakes to debris flows assuming that ground vibrations from an earthquake cause similar damage to a building as vibratory forces from a debris flow impact. Jakob et al. (2012) suggested a damage probability matrix for debris flows based on 68 well-documented case studies worldwide. Four damage classes were related to an intensity index composed of the product of the square of the maximum flow velocity and the maximum expected flow depth. The method was tested on a debris flow event in Italy and exemplarily used to predict the total loss of a 500-year debris flood in a Canadian test site.

The vulnerability functions presented in the literature are developed for different torrent processes and in general residential buildings. Our paper advances previously published results (Fuchs et al., 2007a; Totschnig et al., 2011; Totschnig and Fuchs, 2012). A GIS-based analysis of individual torrent events was conducted to compare vulnerability values for different torrent processes as well as different building types, and to obtain a joint vulnerability function for different torrent processes and different building types exposed. Furthermore, a validation procedure was conducted to show the broader applicability.

2. Test sites

Event data classified as fluvial sediment transport processes and debris flows of five test sites in the Austrian Alps were included in this study and the results were validated by using data from a debris flow event in the Italian Alps. The events in the Austrian test sites were documented immediately after the events by the Institute of Mountain Risk Engineering at the University of Natural Resources and Life Sciences, Vienna on behalf of the Austrian Torrent and Avalanche Control Service. For the selected catchments, data regarding the incurring process type, the process intensity, the damage pattern and the monetary loss were collected. The general morphometric parameters of the Austrian test sites are given in Table 2 and the location of the test sites is shown in Fig. 1.

The test sites Fimbabach, Schnannerbach and Stubenbach are situated in the western part of Austria. The Fimbabach (municipality of Ischgl; Silvretta mountain range) and the Stubenbach (municipality of Pfunds; Samnaun mountain range) are located within the so-called "Engadiner Fenster", a Mesozoic ocean basin which was lifted and reversely faulted by an older unit (Silvretta and Ötztal crystalline). Both torrents are mainly characterised by fluvial sediment transport as the predominant process. The catchment of Schnannerbach is located in the municipality of Pettneu am Arlberg and is part of the Lechtaler Alps, which lithologically comprises mainly dolomite, limestone, marl, sandstone and shale. The Schnannerbach torrent is characterised by fluvial sediment transport and debris floods. All three test sites were affected by the well-documented event of 22 August 2005 (Figure 2) which was consequently used for this study.

The Vorderbergerbach torrent is located in the Southern Austrian Alps. The dominant lithology of the basin is part of the Northern Carnic Alps and comprises mainly limestone and Ordovician shale. Unconsolidated sediment of Quaternary age can be found in the lower parts of the catchment, whereas the upper parts are covered by glacial deposits from the age of the Wurm glaciation. The Vorderbergerbach torrent is prone to fluvial sediment transport. Due to the availability of respective data, the event of 29 August 2003 was used for this analysis.

The Wartschenbach torrent is located in the Southern Austrian Alps next to the city of Lienz. The catchment is part of the Schober mountain range, an Eastern Alpine crystalline unit. The geology consists mainly of paragneiss, mica slate and interstratified amphibolites. Due to glacial action, the upper catchment is partly water-logged and has debris sources within Quaternary depositions of unconsolidated sediment (ground moraines). This unconsolidated material and the steep gradients in the middle reach (30–40%) lead to a high susceptibility to mass movement processes, in particular debris flows (Fuchs et al., 2007a). The events of 6 August 1995 and 16 August 1997 caused

Table 2
General morphometric parameters of the catchments including Melton number and average fan slope.

Test site	Catchment area (km^2)	Range in elevation (m)	Melton number	Average fan slope (%)
Fimbabach	66.3	1349–3399	0.25	3
Schnannerbach	6.6	1240–2889	0.64	13
Stubenbach	29.5	1011–3035	0.37	10
Vorderbergerbach	25.3	588–2052	0.29	3
Wartschenbach	2.3	678–2217	1.01	16

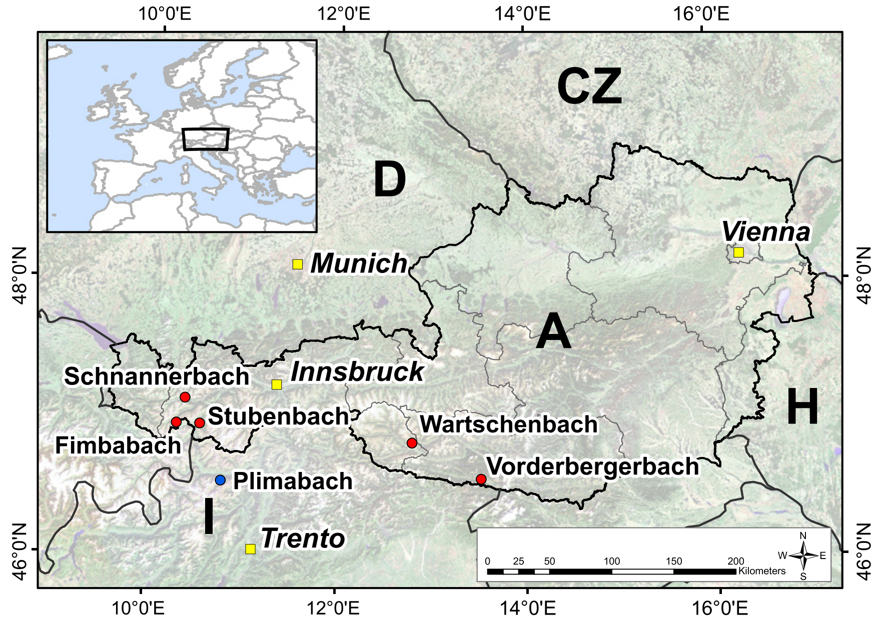

Fig. 1. Location of the test sites in the Austrian Alps, indicated by red dots, and the Italian validation test site, indicated by a blue dot. Layers comprising administrative bodies and shaded relief provided by Environmental Systems Research Institute, Inc. (ESRI).

considerable damage and were therefore well-documented and used for this study.

The Plimabach, located in the Italian validation test site, drains the valley of Martell in the Northern Italian Alps. Lithologically, the basin comprises mainly old crystalline units with quartzite and phyllite in the headwaters and a Permian pluton in the middle reach. The Plimabach flows through the municipality of Martell which was regularly affected by flood events. A reservoir for hydropower generation was built in 1957 in the headwaters of the catchment. Mismanagement and malfunction (power outage) of this reservoir were the main reasons for the severe debris flow event on 24/25 August 1987 (Figure 3). During a period of intense rainfall, a large amount of water (peak discharge of 300–350 m^3/s) was artificially released from the reservoir, which subsequently eroded and transported a considerable amount of sediment downstream (Pfitscher, 1996). The total damage to private and public property in the municipality of Martell summed up to approximately 50 billion Italian Lire (Pfitscher, 1996), which corresponds to approximately € 60 million (in 2012 values).

3. Method

The assessment of risk implies a quantitative assessment of the individual risk components: hazard including temporal and spatial probabilities, elements at risk, and vulnerability. This study focused on the quantification of physical vulnerability of buildings located on torrent fans which were affected by corresponding process intensities. Vulnerability functions, linking the susceptibility of elements at risk to the intensity of the respective hazard processes, were derived. Totschnig et al. (2011) presented a vulnerability function for private residential buildings affected by fluvial sediment transport processes in torrents. Our study was based on these results and pursued the following objectives: Firstly, to include additional data regarding other building types (tourist accommodation) and other process types (debris flows). Secondly, to test the possibility to merge the data based on different processes or building types, and to compute comprehensive vulnerability functions for torrent processes. Thirdly, to validate these vulnerability functions and to demonstrate their applicability in other Alpine areas.

Fig. 2. The event of 22 August 2005, classified as a fluvial sediment transport process, at the Schnannerbach torrent in the municipality of Pettneu am Arlberg (courtesy of ASI Tirol).

Fig. 3. The debris flow event of 24/25 August 1987 at the Plimabach catchment (courtesy of the municipality of Martell).

3.1. Torrent processes

Torrents are defined as constantly or temporarily flowing watercourses with strongly changing perennial or intermittent discharge and flow conditions, originating within small catchment areas (Aulitzky, 1980; Slaymaker, 1988; ONR, 2009). Torrents exhibit a variety of different processes which can be distinguished by the sediment concentration (Costa, 1984) or the peak discharge (Hungr et al., 2001). These processes include pure water flow, fluvial sediment transport, debris floods, and debris flows (Aulitzky, 1980; Costa, 1984; Hungr et al., 2001; ONR, 2009) and are also referred to as hydro-geomorphic processes (e.g., Sakals et al., 2006; Marchi et al., 2010; Jakob et al., 2013). Due to the temporal and spatial variability of sediment concentration during single events the dominant process in the central part of the deposition zone is regularly used to define the entire event characteristics (Hungr et al., 2001). Based on event documentations, dominant processes were assigned to these events. Fluvial sediment transport was found to be the dominant process for the events in the Fimbabach (Hübl et al., 2006), Schnannerbach (Hübl et al., 2006; Chiari and Rickenmann, 2007), Stubenbach (Hübl et al., 2006) and Vorderbergerbach catchments (Hübl et al., 2004). The events in the Wartschenbach torrent were classified as debris flows (Hübl et al., 2002). The event in the Italian validation test site showed, due to the artificial triggering mechanism and the amount of mobilised sediment, debris flow characteristics (compare Figure 3) (Papathoma-Köhle et al., 2012).

An alternative procedure to determine the general predisposition of a catchment for a certain torrent process type was applied (Figure 4). This approach is based on a relation between the Melton number M_E and the average fan slope S_f (Bardou, 2002). In Fig. 4, threshold line A (Marchi and Brochot, 2000; Bardou, 2002) separates fluvial sediment transport processes from mixed processes, whereas threshold line B (Bardou, 2002) separates mixed transport processes from debris flows (Scheidl and Rickenmann, 2010). A Melton number <0.3 is generally seen as an indicator for fluvial sediment transport (Wilford et al., 2004). It is shown in Fig. 4 that the Fimbabach, Stubenbach and Vorderbergerbach catchments are prone to fluvial sediment transport processes due to their low Melton number and their position below or close to the threshold line A. The Wartschenbach torrent is situated in the area of mixed transport processes, but close to threshold line B, indicating the general predisposition for debris flow processes. A clear assignment to a certain process is difficult in case of the Schnannerbach torrent, however, the back-calculated sediment concentration based on water and sediment volume for the studied event is equal to approximately 2% (Chiari and Rickenmann, 2007), confirming the assignment as fluvial sediment transport process.

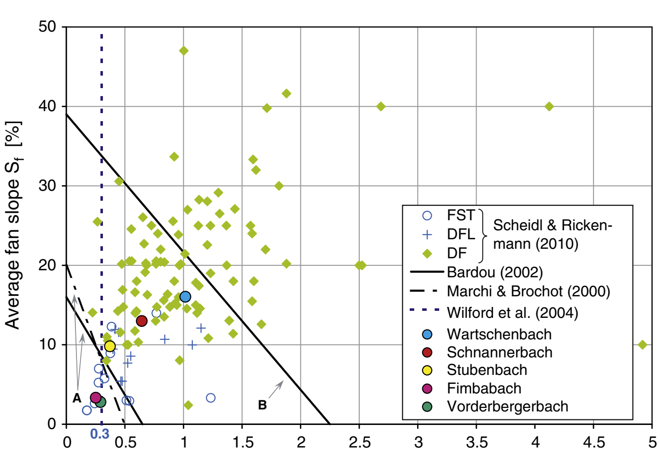

Fig. 4. Relation between average fan slope and Melton number for the five test sites in comparison with results from the literature. Threshold line A separates fluvial sediment transport processes from mixed processes, and threshold line B separates mixed processes from debris flows. The following abbreviations were used: DF = debris flow, DFL = debris flood, FST = fluvial sediment transport, M_E = Melton number, and S_f = average fan slope (modified from Scheidl and Rickenmann, 2010).

3.2. Quantification of vulnerability

Physical vulnerability of buildings is understood as the relation between degree of loss and the corresponding process intensity causing this loss. Degree of loss, partly also referred to as damage ratio, is defined as the ratio between the monetary loss and the reconstruction value of the building. The relation between degree of loss and process intensity can be expressed as a scatterplot of vulnerability values. Using a regression approach, quantitative vulnerability functions were computed from these scatterplots.

3.2.1. Elements at risk

The elements at risk considered within this study included those buildings that were situated on the different torrent fans and were either private residential or tourist accommodation buildings. Reconstruction values for each individual element at risk were calculated using a method adapted from Kranewitter (2002), Keiler (2004) and Keiler et al. (2006). Data regarding the footprint of these buildings were gathered from digital cadastral maps (scale 1:1,000) and multi-temporal aerial photographs. Field studies were necessary to evaluate the number of storeys, the use of storeys, and the state of building maintenance. The state of maintenance was expressed in three classes (good, average and bad state) and included in the calculation of the reconstruction value as a reduction factor (compare Eq. (1) and Table 3). All data were processed and stored in a GIS environment for subsequent computation (e.g., the combination of building location and building address).

The calculation of the reconstruction values for private residential buildings primarily depends on averaged values (unit prices) per m^2 of living space, basement and attic. The averaged values used were those applied by Austrian building insurers in the year 2012 (Table 3), which were considered to be replacement values neglecting any risk-dependent changes in the demand within the real estate market (Fuchs et al., 2007a). Eq. (1) was applied to calculate the reconstruction value of private residential buildings (Totschnig et al., 2011).

$$V_{PR} = 0.9 \cdot A\{U_A + U_B + n_{St}[U_L(1-r)]\} \tag{1}$$

where V_{PR} = value of the private residential building; A = footprint of the building (the additional factor of 0.9 acknowledges that due to the size of interior walls the usable area for living has to be reduced by 10%); n_{St} = number of storeys; U = unit price; r = reduction factor for

Table 3
Unit prices including VAT (price level: 2012) and applied ratio for different building types and usage, which were used in the calculation of the reconstruction values. The ratio (using the unit price of living space in a good state equal to 1904 €/m^2 as the basis) is either the reduction factor for the state of maintenance and interior conditions in the case of private residential buildings or the incremental factor for the different types of tourist accommodation buildings.

Building type	Usage	Unit price (€/m^2)	Ratio
Private residential	Living space (good state)	1904	Basis
	Living space (average state)	1523	−20%
	Living space (bad state)	1428	−25%
	Basement	450	–
	Attic	308	–
Tourist accommodation	Living space (holiday home)	2094	+10%
	Living space (guesthouse)	2380	+25%
	Living space (hotel)	2856	+50%
	Basement (without spa)	450	–
	Spa	2109	–
	Attic	308	–

state of maintenance and interior conditions; the indices A, B and L stand for attic, basement and living space, respectively.

A slightly adapted method was applied to tourist accommodation buildings. Firstly, the averaged value per m^2 for living space was higher. This value was recalculated based on a ratio between unit prices for private residential and tourist accommodation buildings derived from Keiler et al. (2006) for different subtypes of tourist accommodation buildings such as holiday homes, guesthouses, and hotels. Secondly, for some of the buildings the existence of a spa in the basement had to be included in the calculation, as the unit price for spas compared to a standard basement is considerable higher (compare Table 3). Therefore, Eq. (2) was applied for tourist accommodation buildings.

$$V_{TA} = 0.9 \cdot (A_A U_A + A_B U_B + A_S U_S + n_{St} A_L U_L f) \tag{2}$$

where V_{TA} = value of the tourist accommodation building; A = footprint of the building (the additional factor of 0.9 acknowledges that due to the size of interior walls the usable area for living has to be reduced by 10%); n_{St} = number of storeys; U = unit price; f = incremental factor for the different types of tourist accommodation buildings; the indices A, B, S and L stand for attic, basement, spa, and living space, respectively.

Loss data, estimated in monetary terms by professional damage appraisers for each building, were obtained from the respective administrative offices of the Austrian Federal States. The estimations of the professional damage appraisers can be seen as consistent and reliable data sets (Merz, 2006). In accordance with the price level of the used unit prices for the calculation of the reconstruction values (see Eqs. (1), (2) and Table 3), the monetary damage caused was indexed to 2012 values.

3.2.2. Process intensity

Higher process intensities lead to higher vulnerabilities or damages, respectively. This widely acknowledged axiom (e.g., UNDRO, 1979; Fell and Hartford, 1997) is fundamental for the development of vulnerability functions, which express a relation between process intensity and the corresponding degree of loss. The process intensities have to be determined individually for each element at risk. In the case of torrent processes, due to the variable sediment concentration, deposition depth has typically been used within empirical studies as a proxy for the process intensity (Fuchs et al., 2007a; Akbas et al., 2009; Tsao et al., 2010). Deposition depths for the individual buildings were taken from event documentations and additional photo documentations which were made available by some of the home owners. Intensity information for buildings not directly assessed during the field campaigns were obtained from a natural neighbour interpolation carried out in a GIS environment. The natural neighbour interpolation uses Voronoi diagrams to select the set of neighbours of the interpolation point as well as to assign corresponding weights. The natural neighbour interpolation was chosen as it performs well in heterogeneously distributed data and as it creates continuous and smooth surfaces apart from discontinuities that already appear in the input data (Ledoux and Gold, 2005).

Since the number of storeys directly affects the value of the building and vulnerability values for buildings depend on the number of storeys, vulnerability functions based on deposition depth may lead to an overestimation of the vulnerability of higher buildings. To avoid the cumbersome formulation of specific vulnerability functions for each typology of building according to the number of storeys, a relative intensity parameter (Totschnig et al., 2011) was additionally applied in this study.

Both intensity parameters were applied separately and the corresponding results were afterwards compared to each other.

3.2.3. Loss functions

In order to link process intensities (plotted on the abscissa) to the corresponding degrees of loss (plotted on the ordinate) by loss functions, nonlinear regression was applied. Functions were determined by the highest correlation coefficient. The parameters of these functions were estimated by using a sequential quadratic programming (SQP) algorithm based on a nonlinear least squares estimation. SQP is an iterative method for nonlinear optimization that uses the solution of subproblems, which are relatively easy to solve but still can reflect the nonlinearities of the original problem, to construct better approximations (Boggs and Tolle, 1995). As main mathematical requirements the applied cumulative distribution functions (1) define the degree of loss as the dependent variable in a confined interval [0;1] and (2) are steady and monotonic increasing within the interval of its explaining variable (intensity). Table 4 summarises the applied distributions within the nonlinear regression approach. To introduce further parameters, which allow a better fit of the chosen approaches to the given data and at the same time avoid an undesirable shift of the entire function, the distributions were extended by the expression $((x + b)/b) - 1$. This expression allows the fitted functions to still go through the point of origin. The Logistic distribution, which does not go through the point of origin, was additionally modified to coincide with a Log-Logistic distribution.

In contrast to deposition depth, relative intensity values are ranging between 0 and 1. Mathematically spoken, relative intensity is a variable defined in a both-sided confined interval [0;1], assuming that a relative intensity value of 1 (implying a complete burying of the building) must lead at the latest to a total loss, defined as a degree of loss equal to 1. To adjust the distributions of Table 4 so that they were also applicable for relative intensity values, a tangent-transformation (Bronštejn et al., 2008) was applied. The term x (representing the intensity) in these distributions was substituted by the term $\tan(x \cdot \pi/2)$ to transform a variable within a left-sided confined interval $[0;+\infty)$ into a variable defined in a both-sided confined interval [0;1). Following this transformation, the distributions of Table 4 can equally be used for the calculation of vulnerability based on normalised relative intensities.

3.3. Validation

The statistical procedures explained in this section were used for two different purposes. Firstly, the possibility was tested to merge different data based on different processes and building types to derive overall vulnerability functions applicable to torrent processes. Therefore, the statistical tests were targeted at comparing the vulnerability functions for private residential buildings affected by fluvial sediment transport processes with data from private residential buildings affected by debris flows (Section 4.1) and with data from tourist accommodation buildings affected by fluvial sediment transport processes (Section 4.2). These data, subsequently called additional data, came from the Austrian test sites. Secondly, the statistical tests were further used to compare the finally derived Austrian vulnerability functions with the Italian data, subsequently called validation data (Section 4.4).

These comparisons were based on the residuals of the regression analysis. A residual is the difference between the data point and the value of the derived regression function and is related to degree of loss. Using parameter constraining during regression, the parameters

Table 4
Functional approaches (basic and modified mathematical notation) for regression analysis of vulnerability. As Frechet distributions with different numbers of parameters are tested, a numeral suffix is used to distinguish between them.

Distribution	Basic mathematical notation	Modified mathematical notation	Interval of explaining variable
Weibull	$1-e^{-ax^c}$	$1-e^{-a\left(\frac{x+b}{b}-1\right)^c}$	$[0;+\infty)$
Exponential	$1-e^{-ax}$	$1-e^{-a\left(\frac{x+b}{b}-1\right)}$	$[0;+\infty)$
Frechet no. 1	$e^{-x^{-a}}$	$e^{-\left(\frac{x+b}{b}-1\right)^{-a}}$	$(0;+\infty)$
Frechet no. 2	$e^{-x^{-a}}$	$e^{-c\left(\frac{x+b}{b}-1\right)^{-a}}$	$(0;+\infty)$
Logistic	$\frac{1}{1+ae^{-bx}}$	$\frac{1}{1+\left(\frac{x+b}{b}-1\right)^{-a}}$	$(0;+\infty)$

Table 5
Date of event, type of process, number of damaged buildings and number of buildings considered in this study for each test site (Processes: DF — Debris flow, FST — Fluvial sediment transport; Building types: PR — Private residential; TA — Tourist accommodation).

Test site	Date of event	Process	Buildings damaged	Buildings considered	
				PR	TA
Fimbabach	22 August 2005	FST	47	–	40
Schnannerbach	22 August 2005	FST	15	10	1
Stubenbach	22 August 2005	FST	60	28	11
Vorderbergerbach	29 August 2003	FST	41	29	1
Wartschenbach	06 August 1995	DF	14	10	–
Wartschenbach	16 August 1997	DF	16	16	–
Total			**193**	**93**	**53**
Plimabach (IT)	24/25 August 1987	DF	61	34	–

of the calculated regression function can be a priori assigned to coincide with the parameters of a predefined function. Doing so, the calculated residuals refer to the predefined function and can be compared afterwards to the original residuals of this predefined function. For the purpose of merging the Austrian data, a nonlinear regression of the additional data was carried out. The parameters of the regression function were a priori assigned to coincide with the parameters of the functions for fluvial sediment transport processes (Totschnig et al., 2011). In case of the validation procedure, a nonlinear regression of the validation data was carried out. The parameters of the regression function were in this case a priori assigned to coincide with the parameters of the final Austrian vulnerability functions.

The residuals were further compared to the original residuals applying different statistical tests. Statistical hypothesis tests need the determination of a critical significance level (p-value) to prove or reject the corresponding null hypothesis. The null hypothesis typically corresponds to a general statement such as no difference between data sets or no relationship between two parameters. The conventionally applied p-value of 0.05 (Cowles and Davis, 1982; Stigler, 2008) was used in this study as critical significance level. The following statistical tests were applied in this study:

- The Levene's statistic tests the assumption of equal variances by adopting a critical significance level. The result of the Levene's statistic is also needed for the selection of the appropriate independent samples T-test.
- An independent samples T-test compares the residuals regarding their mean values.
- A general linear model in form of an analysis of covariance (ANCOVA) was used to evaluate the influence of a categorical factor (type of process, type of building, and Austrian vs. Italian data) and the covariate intensity on the residuals as the depending variable. In other words, the analysis of covariance was used to test whether or not the residuals are equal across different process and building types as well as across the data of the two studied countries.

Equal variances, equal mean values as well as an insignificant influence of the categorical factor, all of them confirmed by a p-value greater than 0.05, would prove that the tested vulnerability function (the functions for fluvial sediment transport or the final Austrian functions) also fits well to the additional (validation) data. Apart from these statistical tests, the correlation coefficient of the additional (validation) data was calculated and compared to the original one. A high correlation coefficient shows the suitability of the tested vulnerability function to represent the additional (validation) data.

3.4. Estimation of uncertainty

Quantitative vulnerability assessment allows for the estimation of uncertainty inherent to regression functions with confidence intervals. As nonlinear regression functions were calculated, a linear transformation was used (Plate, 1993). The linear transformation approach was based on three steps. Firstly, the functions were converted into a linear form. Secondly, confidence bands with different confidence levels (in this case 90, 95 and 99%) were calculated. Thirdly, the linear confidence bands were transformed back to fit to the original regression functions and then illustrated in the corresponding scatterplots.

The linear transformation approach necessitates, at least for the nonlinear regression functions tested in this study, an approximation of a degree of loss value equal to 1. Due to the mathematical transformations applied, intermediate values of the calculation might not be computable for a degree of loss value equal to 1. Therefore, in this study the degree of loss values equal to 1 were approximated for the estimation of uncertainty by a value of 0.9999. The transformation results are to a certain extent sensitive to the approximation used (e.g., 0.9999 compared to 0.99). However, as only two buildings in this study suffered a degree of loss equal to 1, a comparison of different approximations showed insignificant differences.

4. Results

The number of damaged buildings and their allocation to building types varies across the test sites. Additionally, not all damaged buildings fulfilled the necessary data requirements such as belonging to one of the two studied building types, quantitative registration of the damage in terms of monetary loss as well as assessable deposition depth. A total of 93 private residential and 53 tourist accommodation buildings fulfilled the data requirements in the Austrian test sites. The event in the Italian validation test site caused damage to 61 buildings. 34 buildings, all of them private residential, were used in this study (Table 5).

The following numbers refer to the considered buildings in this study. The reported loss for the Austrian test sites summed up to € 25.8 million. The total property value expressed as reconstruction value was € 191.9 million. The severity of building damage varied between € 499 and € 2.7 million, due to different intensities and different building types affected. Property values of the individual buildings varied between € 252,000 and € 10.8 million. These variations in the amount of reported losses and property values lead to individual

Table 6
Reported loss, property value, range of vulnerability and mean vulnerability for each test site, based on the considered buildings. The values are inflation-adjusted to the year 2012.

Test site	Reported loss (€)	Property value (€)	Range of vulnerability	Mean vulnerability
Fimbabach	11,360,010	87,058,177	0.002–0.656	0.152
Schnannerbach	480,928	7,425,126	0.005–0.171	0.051
Stubenbach	11,423,257	62,554,726	0.013–1.0	0.320
Vorderbergerbach	384,441	22,160,697	0.001–0.050	0.018
Wartschenbach (1995)	559,906	4,964,398	0.010–0.344	0.121
Wartschenbach (1997)	1,639,292	7,745,272	0.006–0.570	0.213
Total	**25,847,834**	**191,908,396**	**0.001–1.0**	**0.166**
Plimabach (IT)	2,402,124	10,881,670	0.026–1.0	0.352

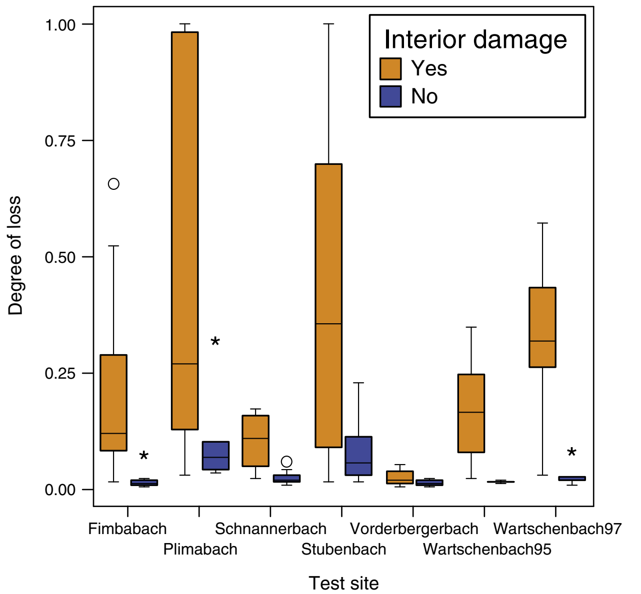

Fig. 5. Box plots which highlight the range in the vulnerability values of the different test sites (orange: damage to the building envelope and interior damage; blue: damage to the building envelope only; circle: outlier between 1.5 and 3 interquartile ranges; asterisk: extreme outlier outside of 3 interquartile ranges).

building vulnerabilities ranging from 0.001 to 1.0. The mean vulnerability per exposed building was equal to 0.166. An overview on these values and the corresponding values for the Italian test site is given in Table 6. In Fig. 5, box plots are shown – distinguishing between buildings with and without interior damage – which highlight the range in the vulnerability values of the different test sites.

In the following figures, vulnerability functions are shown either based on deposition depths (Figures 6a, 7a, 8 and 11a) or relative process intensities (Figures 6b, 7b, 9, 10 and 11b). The process intensity is plotted on the abscissa, and the degree of loss is plotted on the ordinate. Deposition depths are grouped in steps of 0.25 and 0.5 m, respectively. Since the tourist accommodation buildings assessed were only damaged by fluvial sediment transport processes (compare Table 5), a separate comparison between different building types and different processes was undertaken.

4.1. Fluvial sediment transport vs. debris flows

In Fig. 6, the vulnerability functions for fluvial sediment transport and private residential buildings are shown, together with the corresponding vulnerability values and additional vulnerability values for debris flows, based on deposition depths (Figure 6a) or relative intensities (Figure 6b). The results of the statistical tests are given in Table 7. In the case of deposition depths, a similar, even slightly higher, correlation coefficient for debris flows was achieved compared to the correlation coefficient of the vulnerability function for fluvial sediment transport. The p-values of the statistical test showed, as they were greater than 0.05, that there is no significant difference in the variances (Levene's test) and in the mean values (T-test) of the residuals. The analysis of covariance (ANCOVA) confirmed that the type of process did not influence the residuals. In the case of relative intensities, the correlation coefficient of the vulnerability values for debris flows was smaller than the one for fluvial sediment transport (Table 7). The p-values of the statistical test showed that there

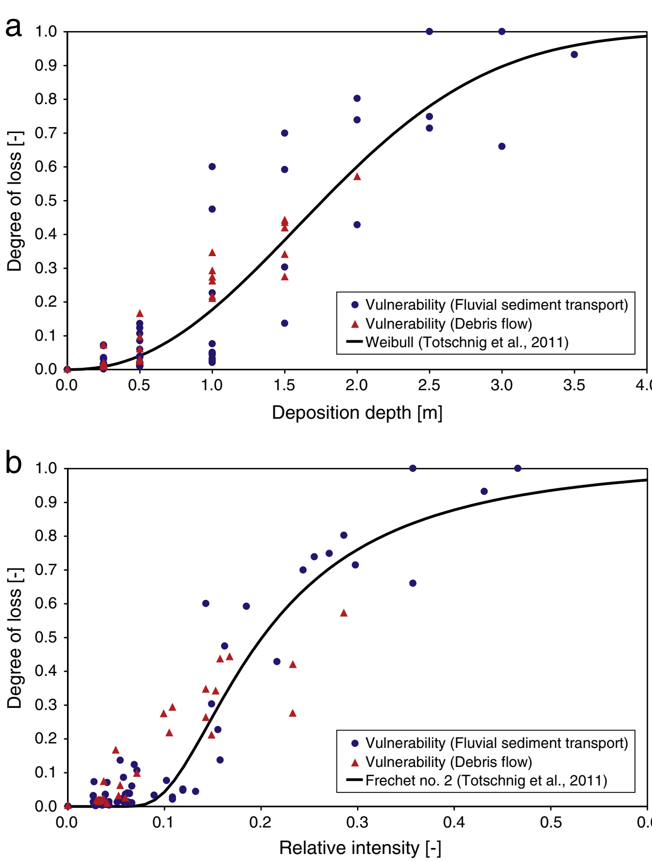

Fig. 6. Vulnerability functions for fluvial sediment transport, together with the corresponding vulnerability values (blue dots) and additional vulnerability values for debris flows (red triangles) based on deposition depths (a) and relative process intensities (b).

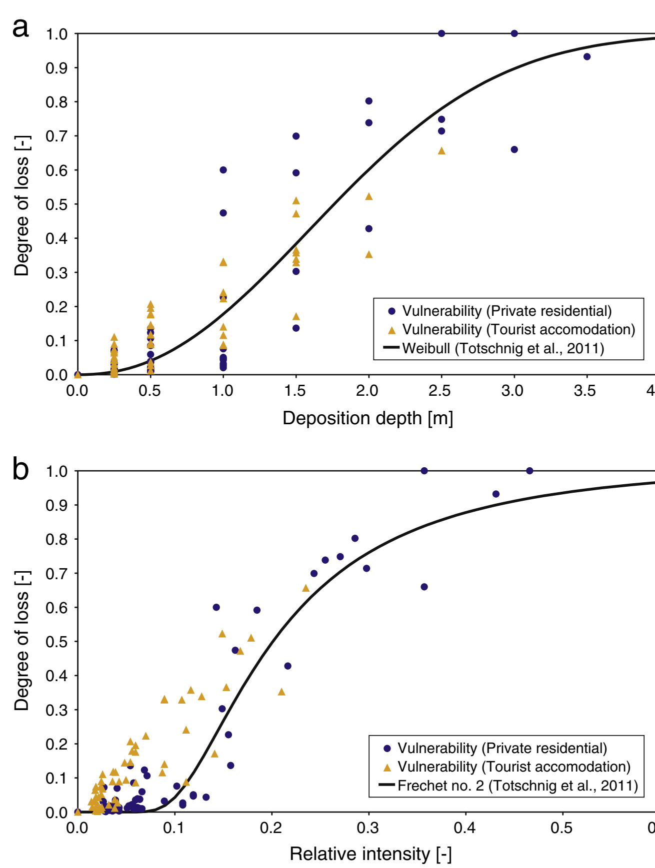

Fig. 7. Vulnerability functions for private residential buildings, together with the corresponding vulnerability values (blue dots) and additional vulnerability values for tourist accommodation buildings (orange triangles) based on deposition depths (a) and relative process intensities (b).

Table 7
Results of the statistical tests for the comparison between different processes (fluvial sediment transport *FST* and debris flow *DF*) based on deposition depths and relative process intensities. The applied significance level (p-value) was equal to 0.05.

Intensity parameter	Correlation coefficient (FST)	Correlation coefficient (DF)	Levene's test (p-value)	T-test (p-value)	ANCOVA (p-value)
Deposition depth	0.914	0.926	0.127	0.322	0.325
Relative intensity	0.958	0.735	0.052	0.572	0.706

is no significant difference in the variances (Levene's test) and in the mean values (T-test) of the residuals. The analysis of covariance confirmed that the type of process did not influence the residuals. Based on these statistical results, a merging (pooling) of the vulnerability values of the two processes based on deposition depths as well as relative intensities and the calculation of joint vulnerability functions is recommended (see Section 4.3).

The analysis of covariance also confirmed for deposition depth (p-value equal to 0.969) as well as relative intensity (p-value equal to 0.275) that the intensity parameter did not influence the residuals.

4.2. Private residential vs. tourist accommodation buildings

In Fig. 7, the vulnerability functions for fluvial sediment transport and private residential buildings are shown, together with the corresponding vulnerability values and additional vulnerability values for tourist accommodation buildings, based on deposition depth (Figure 7a) or relative intensities (Figure 7b). In Table 8, the results of the statistical tests are provided. In the case of deposition depths, the correlation coefficient of the vulnerability values for tourist accommodation buildings was smaller than the one for private residential buildings. The p-values of the statistical test showed, as they were greater than 0.05, that there is no significant difference in the variances (Levene's test) and in the mean values (T-test) of the residuals. The analysis of covariance (ANCOVA) confirmed that the type of building did not influence the residuals. Based on these statistical results, a merging (pooling) of the vulnerability values of the two building types based on deposition depths and the calculation of a joint vulnerability function is recommended (see Section 4.3). In the case of relative intensities, however, the merging (pooling) of vulnerability values of the two building types was not possible. The correlation coefficient of the vulnerability values for tourist accommodation buildings was considerable smaller than the one for private residential buildings. The p-value of the Levene's test showed that there was a significant difference in the variances of the residuals, as it was smaller than 0.05. The p-value of the T-test even confirmed a highly significant difference in the mean values, as it was smaller than 0.01 (Table 8). Similarly, the analysis of covariance also proved that the type of building influences (with a high level of significance) the residuals. Therefore, based on relative intensities and in contrast to absolute deposition depths, an individual vulnerability function for tourist accommodation buildings is recommended to be used (see Section 4.3).

The analysis of covariance confirmed for deposition depth (p-value equal to 0.121) as well as relative intensity (p-value equal to 0.550) that the intensity parameter did not influence the residuals.

Table 8
Results of the statistical tests for the comparison between different building types (private residential *PR* and tourist accommodation *TA*) based on deposition depth and relative process intensities. The applied significance level (p-value) was equal to 0.05.

Intensity parameter	Correlation coefficient (PR)	Correlation coefficient (TA)	Levene's test (p-value)	T-test (p-value)	ANCOVA (p-value)
Deposition depth	0.914	0.826	0.583	0.357	0.428
Relative intensity	0.958	0.540	0.025	<0.001	<0.001

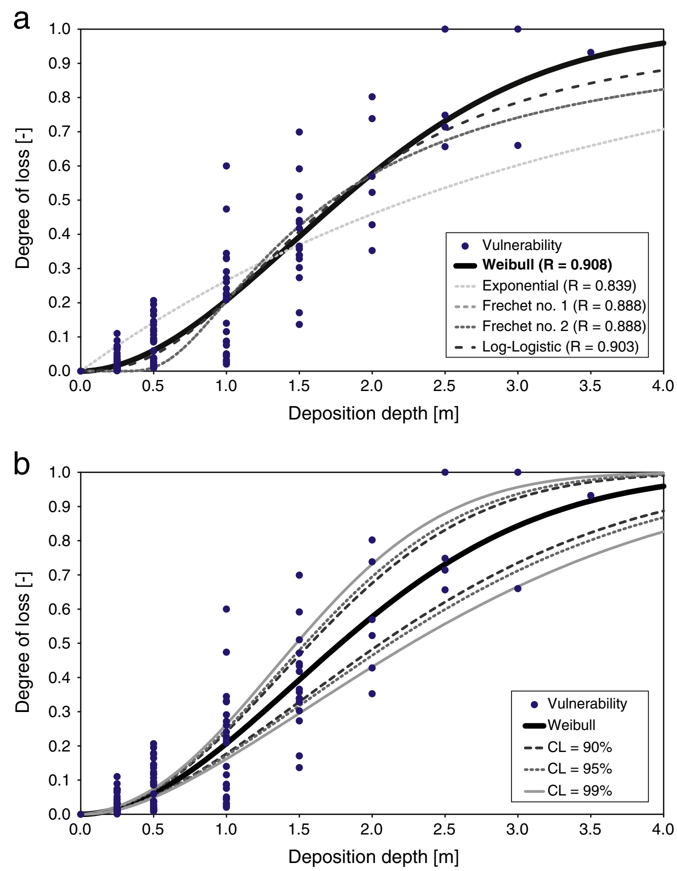

Fig. 8. Different vulnerability functions for the merged data (both processes and both building types), based on deposition depth as a proxy for the process intensity. Vulnerability values originating from the Austrian study sites are indicated by dots. The best-fitting function to describe the range in the analysed data (highest correlation coefficient; Weibull distribution) is highlighted in bold (a). Confidence bands for different confidence levels (CL = 90, 95 and 99%) for the best-fitting function (b).

4.3. Merging vulnerability functions

Due to the statistical results presented in Sections 4.1 and 4.2, a pooling of the vulnerability values of the two processes and the two building types and the calculation of a joint vulnerability function based on deposition depths is recommended. In Fig. 8a, the tested distributions for the merged data set are shown. The best-fitting function to describe the merged data was the Weibull distribution (see Eq. (3)), which is highlighted in Fig. 8a (highest correlation coefficient, equal to 0.908).

$$V_E = 1 - e^{-1.253\left(\frac{I+2.438}{2.438}-1\right)^{1.892}} \tag{3}$$

where V_E = economic vulnerability and I = deposition depth.

Based on relative intensities, the statistical tests presented in Sections 4.1 and 4.2 showed that a joint vulnerability function for residential buildings affected either by fluvial sediment transport processes or debris flows can be proposed. However, in contrast to absolute deposition depths, an individual vulnerability function is recommended to be used for tourist accommodation buildings. In Fig. 9a, the tested distributions for private residential buildings are shown. The best-fitting function to describe the merged data was the Log-Logistic distribution (see Eq. (4)), which is highlighted in Fig. 9a (highest correlation coefficient, equal to 0.941). In Fig. 10a, the tested distributions for tourist accommodation buildings are shown. The best-fitting function to describe the data was the Weibull distribution (see Eq. (5)), which is highlighted in Fig. 10a (the one with the highest correlation coefficient, equal to 0.901). The range of the abscissa in Fig. 10 was kept

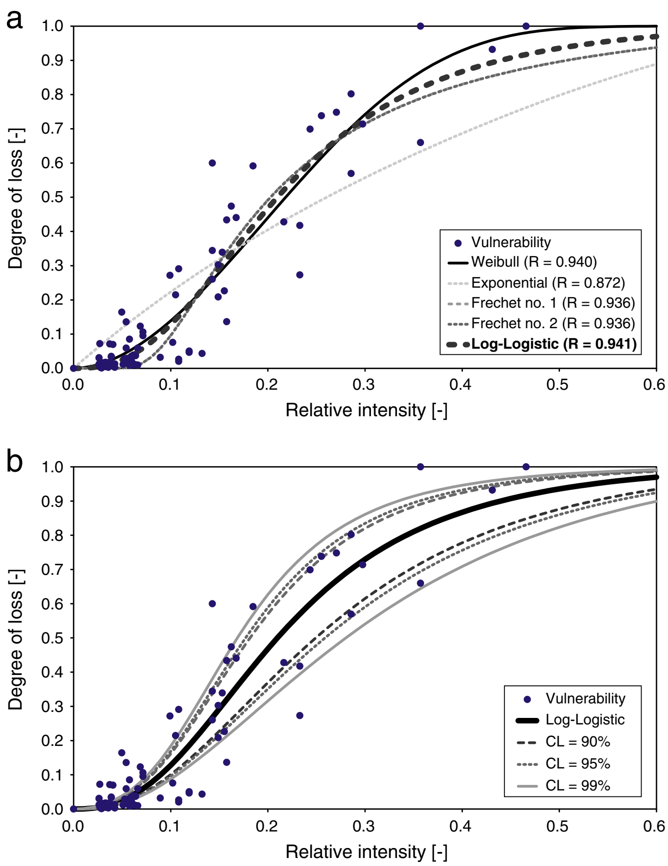

Fig. 9. Different vulnerability functions for the merged data (both processes, private residential buildings), based on relative intensity. Vulnerability values originating from the Austrian study sites are indicated by dots. The best-fitting function to describe the range in the analysed data (highest correlation coefficient; Log-Logistic distribution) is highlighted in bold (a). Confidence bands for different confidence levels (CL = 90, 95 and 99%) for the best-fitting function (b).

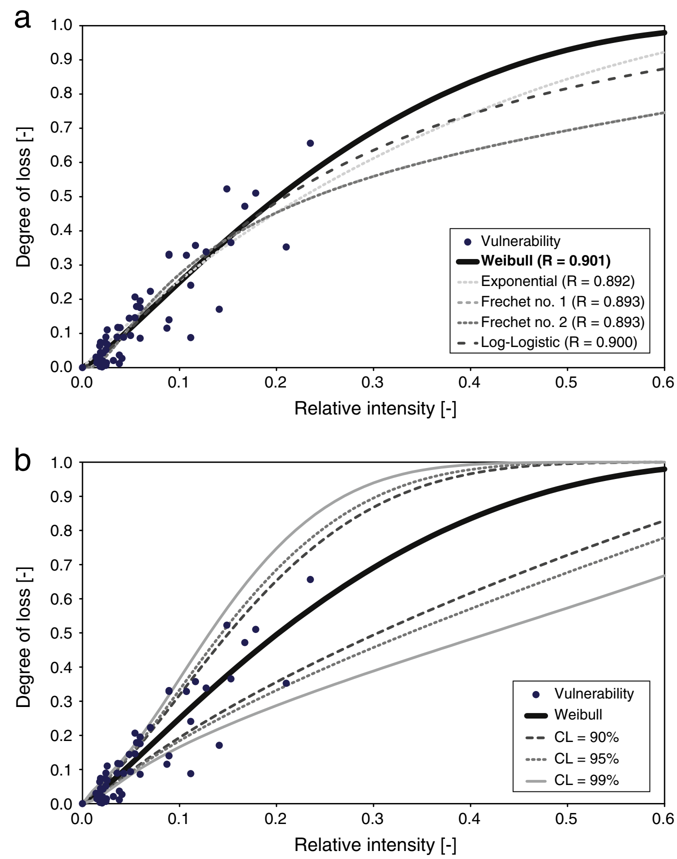

Fig. 10. Different vulnerability functions for tourist accommodation buildings, based on relative intensity. Vulnerability values originating from the Austrian study sites are indicated by dots. The best-fitting function to describe the range in the analysed data (highest correlation coefficient; Weibull distribution) is highlighted in bold (a). Confidence bands for different confidence levels (CL = 90, 95 and 99%) for the best-fitting function (b).

between 0 and 0.6 for comparability purpose. However, the extrapolation of the function beyond an intensity value of 0.23 was not supported with corresponding data and should therefore be re-confirmed by additional studies.

$$V_E = \frac{1}{1+\left(\frac{\tan(I_R\cdot\pi/2)+0.342}{0.342}-1\right)^{-2.492}} \tag{4}$$

$$V_E = 1-e^{-1.254\left(\frac{\tan\left(\frac{I_R\cdot\pi}{2}\right)+0.538}{0.538}-1\right)^{1.205}} \tag{5}$$

where V_E = economic vulnerability and I_R = relative intensity.

In all figures, vulnerability generally increases with increasing intensity and converges towards 1 for high process intensities. The Weibull, Frechet and Log-Logistic distributions show a similar shape in Figs. 8 and 9. A slow increase in vulnerability is observed for low and high process intensities (1 m > I or I > 2.5 m for deposition depths and $0.1 > I_R$ or $I_R > 0.3$ for relative intensities). The curves exhibit the highest rate of increase in vulnerability, following an almost linear curve, for medium process intensities (1 m ≤ I ≤ 2.5 m for deposition depths and $0.1 \leq I_R \leq 0.3$ for relative intensities). Due to this specific shape, an increase in process intensities causes more additional damage at medium intensities compared to low and high intensities. A deviation from this pattern is observed for the exponential curve, given the nature of this distribution. In Fig. 10 however, the shape of all distributions is similar. Fig. 10 refers to tourist accommodation buildings based on relative intensity. Due to the higher vulnerability values for low relative intensities (compared to private residential buildings) and the missing high vulnerability values for high process intensities, the highest rate of increase in vulnerability is observed for low to medium process intensities ($I_R < 0.3$). For high process intensities ($I_R > 0.3$), the observed rate of increase in vulnerability decreases.

To quantify the uncertainty inherent in the calculation of the best-fitting function, confidence bands for different confidence levels (90, 95 and 99%) were calculated (Figures 8b, 9b and 10b). The maximum width of the confidence bands was reached for medium process intensities. In this intensity range, a significant statistical spread of the original data was observed and the number of data points was limited. Although the number of data points further decreased for higher process intensities, the width of the confidence bands became smaller again due to the fact that they converge towards 1.

4.4. Validation

The results presented in Section 4.3 are based on test sites in the Austrian Alps. To test the wider applicability of the derived vulnerability functions, data from an event in the Italian Alps were used. The vulnerability function for tourist accommodation buildings based on relative intensity, however, could not be validated, as only residential buildings were damaged in the Italian test site. The validation results for the other two vulnerability functions (private residential and tourist accommodation buildings based on deposition depth

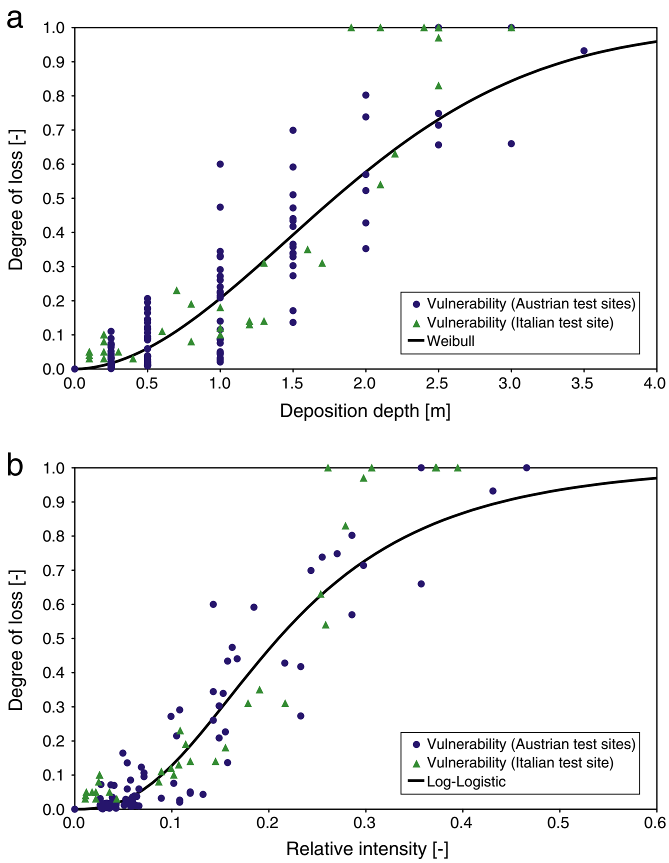

Fig. 11. Best-fitting function for the Austrian test sites based on absolute deposition depths (a) and relative intensity (b), together with the corresponding vulnerability values of the Austrian test sites (blue dots) and vulnerability values of the Italian validation test site (green triangles), see also Papathoma-Köhle et al. (2012).

and private residential buildings based on relative intensity) are summarised in Table 9 and shown in Fig. 11. The correlation coefficients of the validation data were similar to the original ones based on the Austrian data. The p-values of the Levene's test showed that there is a significant difference in the variances of the residuals for both intensity parameters. In case of deposition depth it is even a highly significant difference. The p-values of the T-test proved that there is no significant difference in the mean values. The analysis of covariance confirmed that the differentiation between Austrian and Italian data did not influence the residuals. Although the p-values of the Levene's test showed a significant difference in the variances of the residuals between the Austrian and the Italian data, the high correlation coefficient of the Italian data, the insignificant difference in the mean value of the residuals as well as the insignificant influence of the differentiation between Austrian and Italian data on the residuals lead to the conclusion that the presented functions are also applicable for buildings of the same type in other Alpine regions.

In Table 10, the finally recommended vulnerability functions are summarised, and their most important properties are highlighted.

Table 9
Results of the statistical tests for the validation of the derived Austrian (AUT) vulnerability functions with data from the Italian (IT) test site. The applied significance level (p-value) was equal to 0.05.

Intensity parameter	Correlation coefficient (AUT)	Correlation coefficient (IT)	Levene's test (p-value)	T-test (p-value)	ANCOVA (p-value)
Deposition depth	0.908	0.903	<0.001	0.099	0.059
Relative intensity	0.941	0.943	0.030	0.109	0.132

5. Discussion and conclusion

The presented study extended earlier works (Fuchs et al., 2007a; Totschnig et al., 2011; Totschnig and Fuchs, 2012) on the deduction of empirical vulnerability functions for the physical susceptibility of buildings located on Alpine torrent fans. The considered buildings, private residential and tourist accommodation, were affected in six different torrent events. The events showed process characteristics of either debris flow or fluvial sediment transport. A GIS-based analysis on a local scale (object level) was conducted, defining the degree of loss for each individual building as the ratio between monetary loss and reconstruction value. The reconstruction value was calculated by adopting an insurance approach based on unit prices per m^2 for different building types. The monetary damage was estimated by the respective administrative bodies. To establish vulnerability values for each building the relation between the degree of loss and the corresponding process intensity causing the loss was quantified in a two-dimensional scatter plot. Deposition depth was used as a proxy for process intensity as this intensity parameter is regularly determined in the aftermath of an event. The influence of other intensity parameters such as flow velocity and impact pressure, which were used elsewhere to represent the impact forces (Calvo and Savi, 2009; Quan Luna et al., 2011; Jakob et al., 2012), were not assessed in this study. These parameters could be back-calculated using corresponding models, however using impact pressure or flow velocity for vulnerability functions does not yield necessarily a better correlation (Quan Luna et al., 2011). There is also still a high degree of uncertainty regarding the use of these models (Quan Luna et al., 2011), as well as a high variability of these parameters during the event. By using statistical tests the potential of merging vulnerability values for different torrent processes and building types was tested. Applying a nonlinear regression approach, three final vulnerability functions were proposed. To demonstrate the broader applicability of the results, two of these functions were subsequently validated by using data from an Italian test site.

Statistical tests confirmed that a merging of vulnerability values based on different torrent processes and building types is recommended for absolute intensities (deposition depths). However, for deposition depths between 1.0 and 1.5 m, the statistical spread of the vulnerability values was considerable. This spread may be attributed to a possible intrusion of material through building openings such as windows and doors (Fuchs et al., 2007a; Holub et al., 2012). In this study, however, all buildings affected by an intensity >1 m suffered interior damage with different severity. Hypothesis testing of this issue was not feasible due to the insufficient breakdown of the damage data. This spread may also be attributed to the use of a single intensity parameter as well as the non-consideration of a possible influence of erosive processes. Moreover, the possible influence of different grain size distributions of the deposited sediment on the degree of loss was also not assessed. Nevertheless, a muddy torrent process as in the Vorderbergerbach test site caused the smallest vulnerability values of all test sites. As only small process intensities occurred in the Vorderbergerbach test site ($I \leq 1$ m and $I_R < 0.14$) and no information regarding grain size distribution of the different studied events is available, no general conclusions can be drawn. However, coarser particles might have a more destructive impact on the building envelope and might lead to higher vulnerabilities, at least for small process intensities. A certain degree of scatter can be assigned to the influence of different building heights: there is a statistical correlation between the building height and the degree of loss within individual intensity classes. This correlation is even significant for the deposition depth class of 0.5 m in case of tourist accommodation buildings and 1.0 m in case of private residential buildings. Due to this correlation, a relative intensity, composed from a ratio between deposition depth and the height of the affected building, was applied in this study following a suggestion by Totschnig et al.

Table 10
Compilation of the final vulnerability functions and their range of application (processes: DF — Debris flow, FST — Fluvial sediment transport; building types: PR — Private residential, TA — Tourist accommodation).

Process	Intensity	Building type	Distribution	Mathematical notation	Correlation coefficient	Validation
DF/FST	Absolute	PR/TA	Weibull	$V_E = 1 - e^{-1.253\left(\frac{I+2.438}{2.438}-1\right)^{1.892}}$	0.908	Yes
DF/FST	Relative	PR	Log-Logistic	$V_E = \frac{1}{1+\left(\frac{\tan(I_R\cdot\pi/2)+0.342}{0.342}-1\right)^{-2.492}}$	0.941	Yes
FST	Relative	TA	Weibull	$V_E = 1 - e^{-1.254\left(\frac{\tan\left(\frac{I_R\cdot\pi}{2}\right)+0.538}{0.538}-1\right)^{1.205}}$	0.901	No

(2011). In the case of relative intensity, however, the vulnerability of tourist accommodation buildings exhibited a mismatch compared to private residential buildings. The normalisation of intensity was based on the premise of similar damage potential per affected storey. Tourist accommodation buildings, however, have a higher damage potential in the basement (in case of a spa) and the ground floor (in case of a lounge and of gastronomy) compared to private residential buildings. Furthermore, there is a considerable difference of the mean building height in the test sites between tourist accommodation and private residential buildings (8 to 12 m). These circumstances lead to lower relative intensities but higher degrees of loss compared to deposition depths. Therefore, individual vulnerability functions for private residential and tourist accommodation buildings are proposed.

The uncertainty inherent in the calculation (regression) of all three finally proposed vulnerability functions was quantified by confidence bands. Due to the increased number of data points in the case of merged data the width of the confidence bands was reduced compared to individual data sets. In case of the vulnerability function for tourist accommodation buildings and relative intensity, the confidence band is still considerable wide due to the small amount of data points.

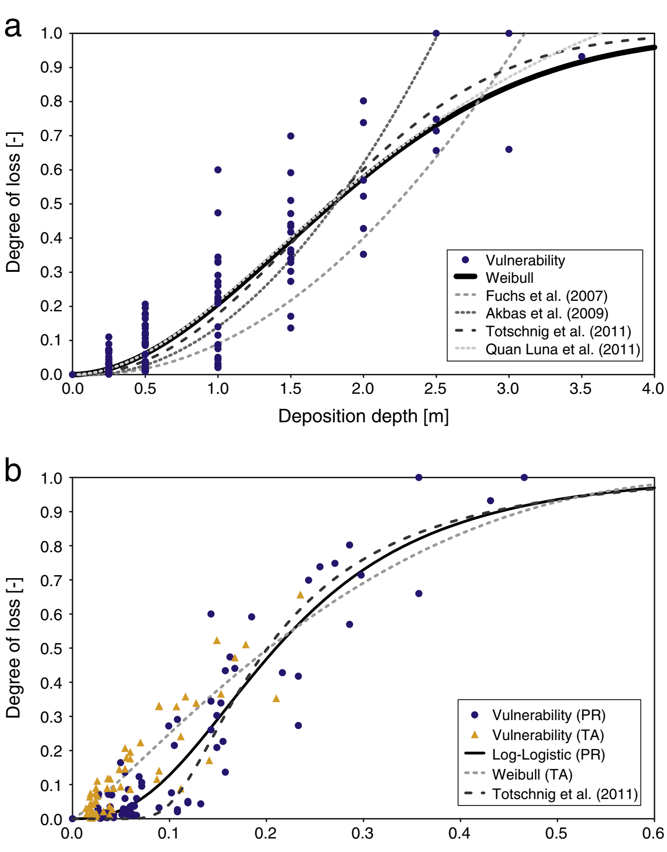

Fig. 12. Comparison of the proposed vulnerability functions with functions presented in the literature based on absolute deposition depths (a) and relative intensity (b). Vulnerability values of the Austrian test sites are either shown all-embracing as blue dots (a) or in case of relative intensity subdivided into private residential (PR) and tourist accommodation buildings (TA) (b).

The validation of the vulnerability functions based on data from the Italian Alps suggested a wider applicability of the presented approach. As shown in Fig. 12a, this applicability is also confirmed by a comparison with different vulnerability functions presented in the literature. Above all, the function reported in Quan Luna et al. (2011) shows a sound fit, whereas the two second order polynomial functions suggested for debris flows (Fuchs et al., 2007a; Akbas et al., 2009) yield in generally lower vulnerability values. Concerning relative intensity, only a limited comparison of vulnerability functions was possible; in Fig. 12b the derived vulnerability functions for private residential and tourist accommodation buildings are compared with those presented by Totschnig et al. (2011). Due to the higher vulnerability values for low relative intensities in case of tourist accommodation buildings, the corresponding vulnerability function showed a higher rate of increase in vulnerability for low process intensities than the other two functions which were derived for private residential buildings. Furthermore, a validation of the vulnerability function for tourist accommodation buildings based on relative process intensities is still outstanding as only residential buildings were included in the Italian data set.

To conclude, the results suggest that there is no need to distinguish between different sediment-laden torrent processes (including debris floods) when assessing physical vulnerability of residential buildings towards torrent processes. However, the differentiation between different types of processes is still necessary for the development of comprehensive mitigation concepts (Hübl et al., 2011; Mazzorana et al., 2012) and might be necessary for the assessment of the vulnerability of other elements at risk, such as persons or infrastructure. The derived vulnerability functions may be applied within the framework of risk management for mountain hazards within the European Alps. The method is transferable to other alpine regions if the needed input data are available. This data availability, however, may be a major constrain in some countries (e.g., Jakob et al., 2012; Lo et al., 2012). Therefore, more data of well-documented events have to be collected in order to allow for further validation of the results and to support an enhanced standardisation of the vulnerability functions presented.

Acknowledgements

This work was funded by the Austrian Science Fund (FWF: L535-N10). The authors wish to express their sincere thanks to J. van Straaten for helpful comments on an earlier draft of this paper as well as to acknowledge the valuable efforts by two anonymous reviewers for an improvement of the manuscript.

References

Akbas, S.O., Blahut, J., Sterlacchini, S., 2009. Critical assessment of existing physical vulnerability estimation approaches for debris flows. In: Malet, J., Remaître, A., Bogaard, T. (Eds.), Landslide Processes: from Geomorphological Mapping to Dynamic Modelling. CERG Editions, Strasbourg, pp. 229–233.

Alexander, D., 2000. Confronting Catastrophe: New Perspectives on Natural Disasters. Terra Publications, Harpenden.

Aulitzky, H., 1980. Preliminary two-fold classification of torrents. In: Aulitzky, H., Grubinger, H., Nemecek, E. (Eds.), Internationales Symposion Interpraevent – Bad Ischl (8.-12. September). Internationale Forschungsgesellschaft Interpraevent, Klagenfurt, pp. IV/285–IV/309.

Barbolini, M., Cappabianca, F., Sailer, R., 2004. Empirical estimate of vulnerability relations for use in snow avalanche risk assessment. In: Brebbia, C. (Ed.), Risk Analysis IV. WIT, Southampton, pp. 533–542.

Bardou, E., 2002. Methodologie de diagnostic des laves torrentielles sur un bassin versant alpin. PhD Thesis, École Polytechnique Fédérale de Lausanne, Lausanne, p. 171.

Bell, R., Glade, T., 2004. Quantitative risk analysis for landslides — examples from Bíldudalur, NW-Iceland. Natural Hazards and Earth System Sciences 4, 117–131.

Boggs, P.T., Tolle, J.W., 1995. Sequential quadratic programming. Acta Numerica 4, 1–51.

Borter, P., 1999a. Risikoanalyse bei gravitativen Naturgefahren — Methode. Bundesamt für Umwelt, Wald und Landschaft, Bern.

Borter, P., 1999b. Risikoanalyse bei gravitativen Naturgefahren — Fallbeispiele und Daten. Bundesamt für Umwelt, Wald und Landschaft, Bern.

Bronštejn, I.N., Semendjajew, K.A., Musiol, G., Mühlig, H., 2008. Taschenbuch der Mathematik. Verlag Deutsch, Frankfurt/Main.

BWW, 1997. Berücksichtigung der Hochwassergefahren bei raumwirksamen Tätigkeiten. Bundesamt für Wasserwirtschaft, Bundesamt für Raumplanung und Bundesamt für Umwelt, Wald und Landschaft, Biel.

Calvo, B., Savi, F., 2009. A real-world application of Monte Carlo procedure for debris flow risk assessment. Computers & Geosciences 35, 967–977.

Carter, W., 1992. The disaster management cycle. In: Carter, W. (Ed.), Disaster Management: A Disaster Manager's Handbook. Asian Development Bank, Manila, pp. 51–59.

Cendrero, A., Remondo, J., Bonachea, J., Rivas, V., Soto, J., 2006. Sensitivity of landscape evolution and geomorphic processes to direct and indirect human influence. Geografia Fisica e Dinamica Quaternaria 29, 125–137.

Chiari, M., Rickenmann, D., 2007. The influence of form roughness on modelling sediment transport at steep slopes. In: Kostadinov, S., Bruk, S., Walling, D. (Eds.), Erosion and torrent control as a factor in sustainable river basin management (Conference Proceedings on CD-ROM), Belgrade.

Costa, J.E., 1984. Physical geomorphology of debris flows. In: Costa, J.E., Fleisher, P. (Eds.), Developments and Applications of Geomorphology. Springer, Berlin, pp. 268–317.

Cowles, M., Davis, C., 1982. On the origins of the .05 level of statistical significance. American Psychologist 37, 553–558.

Faella, C., Nigro, E., 2001a. Effetti delle colate rapide sulle costruzioni. Parte prima: descrizione del danno. Meeting on Il rischio idrogeologico in Campania – Fenomeni di colata rapida di fango nel maggio '98. Commissariato di Governo per l'emergenza idrogeologica in Campania, pp. 102–112.

Faella, C., Nigro, E., 2001b. Effetti delle colate rapide sulle costruzioni. Parte seconda: valutazione della velocità d'impatto. Meeting on Il rischio idrogeologico in Campania – Fenomeni di colata rapida di fango nel maggio '98. Commissariato di Governo per l'emergenza idrogeologica in Campania, pp. 113–125.

Fell, R., Hartford, D., 1997. Landslide risk management. In: Cruden, D., Fell, R. (Eds.), Landslide Risk Assessment. Balkema, Rotterdam, pp. 51–109.

Fell, R., Corominas, J., Bonnard, C., Cascini, L., Leroi, E., Savage, W.Z., 2008. Guidelines for landslide susceptibility, hazard and risk zoning for land use planning. Engineering Geology 102, 85–98.

FEMA, 2007. Multi-hazard loss estimation methodology: Flood model HAZUS^{MH} MR3. Department of Homeland Security, Federal Emergency Management Agency, Washington, DC.

Fuchs, S., 2009. Susceptibility versus resilience to mountain hazards in Austria — paradigms of vulnerability revisited. Natural Hazards and Earth System Sciences 9, 337–352.

Fuchs, S., Heiss, K., Hübl, J., 2007a. Towards an empirical vulnerability function for use in debris flow risk assessment. Natural Hazards and Earth System Sciences 7, 495–506.

Fuchs, S., Thöni, M., McAlpin, M.C., Gruber, U., Bründl, M., 2007b. Avalanche hazard mitigation strategies assessed by cost effectiveness analysis and cost benefit analysis — evidence from Davos, Switzerland. Natural Hazards 41, 113–129.

Fuchs, S., Kuhlicke, C., Meyer, V., 2011. Vulnerability to natural hazards — the challenge of integration. Natural Hazards 58, 609–619.

Fuchs, S., Ornetsmüller, C., Totschnig, R., 2012. Spatial scan statistics in vulnerability assessment — an application to mountain hazards. Natural Hazards 64, 2129–2151.

Haugen, E.D., Kaynia, A.M., 2008. Vulnerability of structures impacted by debris flow. In: Chen, Z., Zhang, J.-M., Ho, K., Wu, F.-Q., Li, Z.-K. (Eds.), Landslides and Engineered Slopes. Taylor & Francis, London, pp. 381–387.

Holub, M., Fuchs, S., 2009. Mitigating mountain hazards in Austria — legislation, risk transfer, and awareness building. Natural Hazards and Earth System Sciences 9, 523–537.

Holub, M., Gruber, H., Fuchs, S., 2011. Naturgefahren-Risiko aus Sicht des Versicherers. Wildbach- und Lawinenverbau 167, 74–86.

Holub, M., Suda, J., Fuchs, S., 2012. Mountain hazards: reducing vulnerability by adapted building design. Environmental Earth Sciences 66, 1853–1870.

Hu, K.H., Cui, P., Zhang, J.Q., 2012. Characteristics of damage to buildings by debris flows on 7 August 2010 in Zhouqu, Western China. Natural Hazards and Earth System Sciences 12, 2209–2217.

Hübl, J., Ganahl, E., Moser, M., Schnetzer, I., 2002. Dokumentation Wartschenbach. WLS Report 52. Institut für Alpine Naturgefahren, Universität für Bodenkultur, Wien, p. 75.

Hübl, J., Leber, D., Brauner, M., Janu, S., Volk, G., Holzinger, H., Gruber, H., 2004. Dokumentation der Unwetterereignisse in den Gemeinden St. Stefan/Vorderberg und Feistritz an der Gail vom 29. August 2003. WLS Report 99. Institut für Alpine Naturgefahren, Universität für Bodenkultur, Wien, p. 78.

Hübl, J., Ganahl, E., Bacher, M., Chiari, M., Holub, M., Kaitna, R., Prokop, A., Dunwoody, G., Forster, A., Schneiderbauer, S., 2006. Dokumentation der Wildbachereignisse vom 22./23. August 2005 in Tirol — Detaillierte Aufnahme. IAN Report 109. Institut für Alpine Naturgefahren, Universität für Bodenkultur, Wien, p. 73.

Hübl, J., Fuchs, S., Sitter, F., Totschnig, R., 2011. Towards a frequency-magnitude relationship for torrent events in Austria. In: Genevois, R., Hamilton, D.L., Prestininzi, A. (Eds.), 5th International Conference on Debris-flow Hazards Mitigation: Mechanics, Prediction and Assessment. Casa Editrice Università La Sapienza, Padua, pp. 895–902.

Hungr, O., Evans, S.G., Bovis, M.J., Hutchinson, J.N., 2001. A review of the classification of landslides of the flow type. Environmental and Engineering Geoscience 7, 221–238.

Jakob, M., Lambert, S., 2009. Climate change effects on landslides along the southwest coast of British Columbia. Geomorphology 107, 275–284.

Jakob, M., Stein, D., Ulmi, M., 2012. Vulnerability of buildings to debris flow impact. Natural Hazards 60, 241–261.

Jakob, M., Holm, K., Weatherly, H., Liu, S., Ripley, N., 2013. Debris flood risk assessment for Mosquito Creek, British Columbia, Canada. Natural Hazards 65, 1653–1681.

Keiler, M., 2004. Development of the damage potential resulting from avalanche risk in the period 1950–2000, case study Galtür. Natural Hazards and Earth System Sciences 4, 249–256.

Keiler, M., Zischg, A., Fuchs, S., 2006. Methoden zur GIS-basierten Erhebung des Schadenpotenzials für naturgefahreninduzierte Risiken. In: Strobl, J., Roth, C. (Eds.), GIS und Sicherheitsmanagement. Wichmann, Heidelberg, pp. 118–128.

Keiler, M., Knight, J., Harrison, S., 2010. Climate change and geomorphological hazards in the eastern European Alps. Philosophical Transactions of the Royal Society A 368, 2461–2479.

Kienholz, H., Krummenacher, B., Kipfer, A., Perret, S., 2004. Aspects of integral risk management in practice — considerations with respect to mountain hazards in Switzerland. Österreichische Wasser- und Abfallwirtschaft 56, 43–50.

Kranewitter, H., 2002. Liegenschaftsbewertung, 4th ed. Gesco, Wien.

Ledoux, H., Gold, C., 2005. An efficient natural neighbour interpolation algorithm for geoscientific modelling. In: Fischer, P.F. (Ed.), Modelling Developments in Spatial Data Handling. Springer, Berlin, pp. 97–108.

Lo, W.-C., Tsao, T.-C., Hsu, C.-H., 2012. Building vulnerability to debris flows in Taiwan: a preliminary study. Natural Hazards 64, 2107–2128.

Marchi, L., Brochot, S., 2000. Les cônes de déjection torrentiels dans les Alpes françaises: morphométrie et processus de transport solide torrentiel. Revue de Géographie Alpine 88, 23–38.

Marchi, L., Cavalli, M., D'Agostino, V., 2010. Hydrogeomorphic processes and torrent control works on a large alluvial fan in the eastern Italian Alps. Natural Hazards and Earth System Sciences 10, 547–558.

Mazzorana, B., Levaggi, L., Keiler, M., Fuchs, S., 2012. Towards dynamics in flood risk assessment. Natural Hazards and Earth System Sciences 12, 3571–3587.

Merz, B., 2006. Hochwasserrisiken. Schweizerbart, Stuttgart.

ONR, 2009. Schutzbauwerke der Wildbachverbauung — Begriffe und ihre Definitionen sowie Klassifizierung. ONR 24800. Österreichisches Normungsinstitut, Wien.

Papathoma-Köhle, M., Keiler, M., Totschnig, R., Glade, T., 2012. Improvement of vulnerability curves using data from extreme events: debris-flow event in South Tyrol. Natural Hazards 64, 2083–2105.

Pfitscher, A., 1996. Wasserkatastrophen im Martelltal. Athesia, Bozen.

Plate, E.J., 1993. Statistik und angewandte Wahrscheinlichkeitslehre für Bauingenieure. Ernst & Sohn, Berlin.

Quan Luna, B., Blahut, J., Van Westen, C.J., Sterlacchini, S., Van Asch, T.W.J., Akbas, S.O., 2011. The application of numerical debris flow modelling for the generation of physical vulnerability curves. Natural Hazards and Earth System Sciences 11, 2047–2060.

Republik Österreich, 1996. Katastrophenfondsgesetz 1996. BGBl 201/1996, Wien.

Romang, H., 2004. Wirksamkeit und Kosten von Wildbach-Schutzmassnahmen. Verlag des Geographischen Instituts der Universität Bern, Bern.

Sakals, M.E., Innes, J.L., Wilford, D.J., Sidle, R.C., Grant, G.E., 2006. The role of forests in reducing hydrogeomorphic hazards. Forest, Snow and Landscape Research 80, 11–22.

Scheidl, C., Rickenmann, D., 2010. Empirical prediction of debris-flow mobility and deposition on fans. Earth Surface Processes and Landforms 35, 157–173.

Schultz, M.T., Gouldby, B.P., Simm, J.D., Wibowo, J.L., 2010. Beyond the factor of safety: developing fragility curves to characterize system reliability. Water Resources Infrastructure Program. U.S. Army Engineer Research and Development Center, Vicksburg, p. 50.

Slaymaker, O., 1988. The distinctive attributes of debris torrents. Journal of Hydrological Sciences 33, 567–573.

Stigler, S., 2008. Fisher and the 5% level. Chance 21, 12.

Totschnig, R., Fuchs, S., 2012. Vergleich von Vulnerabilitätskurven für Wildbachprozesse. In: Koboltschnig, G., Hübl, J., Braun, J. (Eds.), Internationales Symposion Interpraevent – Grenoble (23.-26. April), vol. 2. Internationale Forschungsgesellschaft Interpraevent, Klagenfurt, pp. 1103–1114.

Totschnig, R., Sedlacek, W., Fuchs, S., 2011. A quantitative vulnerability function for fluvial sediment transport. Natural Hazards 58, 681–703.

Tsao, T.-C., Hsu, W.-K., Cheng, C.-T., Lo, W.-C., Chen, C.-Y., Chang, Y.-L., Ju, J.-P., 2010. A preliminary study of debris flow risk estimation and management in Taiwan. In: Chen, S.-C. (Ed.), International Symposium Interpraevent in the Pacific Rim – Taipei (26.-30. April). Internationale Forschungsgesellschaft Interpraevent, Klagenfurt, pp. 930–939.

UNDRO, 1979. Natural Disasters and Vulnerability Analysis. Department of Humanitarian Affairs/United Nations Disaster Relief Office, Geneva, p. 53.
Uzielli, M., Nadim, F., Lacasse, S., Kaynia, A.M., 2008. A conceptual framework for quantitative estimation of physical vulnerability to landslides. Engineering Geology 102, 251–256.
Wilford, D.J., Sakals, M.E., Innes, J.L., Sidle, R.C., Bergerud, W.A., 2004. Recognition of debris flow, debris flood and flood hazard through watershed morphometrics. Landslides 1, 61–66.
Zanchetta, G., Sulpizio, R., Pareschi, M.T., Leoni, F.M., Santacroce, R., 2004. Characteristics of May 5–6, 1998 volcaniclastic debris flows in the Sarno area (Campania, southern Italy): relationships to structural damage and hazard zonation. Journal of Volcanology and Geothermal Research 133, 377–393.